VOL. 13 NO. 5,
AUGUST, 2026
E-ISSN 3027-1339
P-ISSN 3026-8257

African Scholar Publications & Research International
www.africanscholarpub.com

Journal of Systematic, Evaluation and Diversity Engr. (JSEDE)

Two-Horizon Deterministic and Probabilistic Screening of Upstream Oil and Gas Pressure Assets under Corrosion-Driven Wall Loss

Amanze Gregory Onwuzurike; Izelu Christopher; John Alabo Michael; & Frank Ihinosen Amedu

Department of Mechanical Engineering, College of Engineering and Technology, Federal, University of Petroleum Resources, Effurun, Delta State, Nigeria.

Corresponding Author: alabojohn17@gmail.com

DOI: https://doi.org/10.70382/ajsede.v13i5.051

Abstract

Corrosion-induced wall loss can substantially reduce the pressure-containment capability of equipment, underscoring the importance of reliable screening for upstream oil and gas assets. However, comparing mechanics-based screening conditions across different pressure assets is challenging, particularly when wall-thickness limits, stress utilisation, and uncertainty must be considered over common future horizons. In this paper, we assess six numerical pressure-asset cases using a deterministic and probabilistic screening framework across two future horizons. The cases comprise a crude-oil pipeline (A1), a gas pipeline (A2), a multiphase flowline (A3), a pressure-separator shell (A4), a compressor-discharge line (A5), and an offshore export pipeline (A6). Remaining wall thickness and mean-diameter hoop-stress utilisation are calculated at the baseline (initial) state and at five- and ten-year horizons. The joint probability of satisfying both minimum wall-thickness and hoop-stress criteria is then estimated using 1,000,000 Monte Carlo realisations per asset, accounting for uncertainties in operating pressure, allowable material resistance, initial wall thickness, and corrosion rate. Estimated ten-year screening reliabilities for assets A1 through A6 are 0.9328, 0.0308, 0.0029, 0.8165, 0.0061, and 0.0049, respectively. An initial stress-limit exceedance is identified for A6 (utilization = 1.008), while the wall thickness of A3 is projected to fall below its specified minimum at ten years. Lowering the joint-efficiency factor for separator A4 from 1.00 to 0.85 reduces its ten-year screening reliability from 0.8165 to 0.1205. The analysis demonstrates that thickness and stress limit states can flag different screening concerns and that relative asset rankings can shift depending on the assessment horizon. This methodology provides an initial basis for prioritizing assets that warrant detailed, component-specific integrity assessment.

Keywords: Corrosion Wall Loss, Pipeline Integrity, Pressure Vessels, Screening Reliability, Monte Carlo Simulation, Inspection Planning.

Introduction

Internal corrosion-induced wall loss has become a critical integrity and resilience challenge across ageing upstream oil and gas facilities, threatening containment safety, operational continuity and financial viability (NACE International, 2016; Pipeline and Hazardous Materials Safety Administration, 2018a). Global corrosion losses remain benchmarked at approximately US$2.5 trillion annually, equivalent to approximately 3.4% of global gross domestic product (GDP) at the 2013 benchmark (NACE International, 2016) while regulatory records from the United States (US) Pipeline and Hazardous Materials Safety Administration (PHMSA) indicate that corrosion accounted for approximately 18% of reported pipeline incidents during 1998–2017, with internal corrosion historically accounting for nearly 60% of corrosion-related incidents on transmission and gathering pipelines (PHMSA, 2018a, 2018b). Because transmission pipelines, multiphase flowlines, compressor piping and separator shells all depend on sufficient wall thickness to contain pressurised fluids, progressive thinning directly erodes structural safety margins across production trains (Hussain et al., 2024; H. Li et al., 2022). Ideally, a uniform set of screening rules would allow operators to rank degradation risk consistently across all pressurised equipment. However, variations in operating loads, weld joint efficiencies, material assumptions and governing design standards such as American Society of Mechanical Engineers (ASME) B31G and Det Norske Veritas Recommended Practice DNV-RP-F101 for pipelines versus ASME Section VIII and American Petroleum Institute (API) Standards 510 and 570 for pressure vessels and process piping cause minimum wall-thickness and hoop-stress screening margins to respond differently over time (API, 2022, 2024; ASME, 2023, 2025; DNV, 2025; Ma et al., 2023). Thus, equipment can pass one short-term inspection, yet show markedly lower screening reliability over longer assessment horizons. The ongoing challenge is that the combined pressure-asset compliance behaviour, inter-horizon reliability deterioration and comparative wall-thickness and hoop-stress hierarchy for dissimilar pressure devices are yet to be satisfactorily modelled across common future assessment horizons, preventing the operator from systematically prioritising further fitness-for-service (FFS) evaluations on mixed equipment portfolios.

The problem remains because current integrity techniques and structural reliability studies base degradation evaluations on incompatible sets of rules, individual-asset scope, or different time frames. Critical deterministic checks in older engineering standards define minimum requirements to separate uniform wall thinning, which increases nominal hoop stress, from localised corrosion and interacting defect clusters, which demand geometry-dependent burst and leakage algorithms (Dao et al., 2023; Velázquez et al., 2022, 2024). Advances in in-line inspection (ILI) data analytics, including automated defect linking, outlier identification and data-driven remaining-life models, have notably improved defect monitoring on single lines (Amaya-Gómez et al., 2022, 2024; Cui & Wang, 2024; Hussain & Zhang, 2025; Pascal, 2026a).

Similarly, approaches based on probabilistic subset simulation models, finite-element modelling of interacting flaws, spatially-dependent system reliability, and risk-based inspection (RBI) planning have shown that different limit states (such as burst and leakage) may dominate at various points during an asset's

service life (Boufkhed et al., 2026; Hsu, 2024; Huang et al., 2023; C. Li et al., 2023; Mensah & Sriramula, 2024; Nahal et al., 2023; Zerouali et al., 2024). These studies have demonstrated how an asset can meet its minimum specified wall thickness yet surpass its permissible hoop stress limits or pass the stress check yet be thinner than minimum wall allowance. However, much of this probabilistic research considers an individual asset class (such as an onshore transmission pipeline) with a different limit state, defect geometry, or period of assessment, and this difference in methodology means that the results cannot be directly compared between facilities with mixed pipeline, flowline, compressor-line and pressure vessel assets, where a constant rate of wall-loss combined with multi-year uncertainty quantification provides a straightforward method of screening at inception (Hsu, 2024; C. Li et al., 2023; Ma et al., 2023).

The research gap identified has led to the need for a standardised multi-horizon, cross-asset deterministic and probabilistic screening standard that considers minimum wall-thickness and hoop-stress limit states independently and in combination across mixed pressure equipment. This necessitates the development of an analytical approach that supports the propagation of the input uncertainties through common future horizons while monitoring inter-horizon reliability decline and changes in portfolio ranking.

In this work, we suggest that stand-alone and ensemble assessments of minimum wall-thickness and mean-diameter hoop-stress criteria at typical future horizons expose separate drivers of failure-mode incidence and portfolio rank reversal with respect to composite inspections that are missed with stand-alone, single-horizon or single-criterion checks. We examine this hypothesis through deterministic and probabilistic screening analysis at two future horizons in six representative numerical pressure assets: a crude-oil transmission pipeline (A1), a gas transmission pipeline (A2), a multiphase flowline (A3), a cylindrical pressure-separator shell (A4), a compressor-discharge line (A5) and an offshore export pipeline (A6). This work is driven by the practical application of a simple transparent Tier-1 portfolio triage mechanism that can represent real-world design, welding, material and corrosion uncertainties. First, wall thinning and hoop-stress utilisation are deterministically assessed at baseline and at five- and ten-year horizons to distinguish likely baseline threshold exceedances and time-dependent wall-loss failures. Second, uncertainties in operating pressure, allowable strength, initial wall thickness and corrosion rate are randomly propagated at 1,000,000 Monte Carlo trials per asset, and the estimated probability of passing both screening limits (reliability) is tracked at the alternative planning horizons to quantify rank reversal through inter-horizon reliability decline (ΔR) and through the rate of decay (k) over the interval. Inter-horizon sensitivity to weld joint efficiency is demonstrated at a single asset. The paper aims to provide simple mechanics-based screening at uniform wall-loss scenarios for these classical upstream oil and gas pressure-assets to establish a baseline for multi-asset integrity prioritisation.

RESEARCH METHODOLOGY

Benchmark Asset Portfolio and Input Parameters

Six numerical pressure-asset benchmarks (A1–A6), representing upstream production, processing and transmission assets, were analysed using a coupled deterministic and probabilistic screening methodology. Table 1 presents the reference outside diameter (D), operating pressure (P), initial wall thickness (t_0), specified minimum screening thickness ($t_{\min}$), allowable screening resistance threshold (S_{allow}), nominal corrosion rate (CR) and inspection interval (I) for each case.

Table 1. Deterministic reference inputs for the six numerical pressure-asset benchmarks

Asset	System	Material	D (mm)	P (MPa)	t_0 (mm)	$t_{\min}$ (mm)	S_{allow} (MPa)	CR (mm/yr)	I (yr)
A1	Crude oil transmission pipeline	API 5L X65	610	8.00	10.80	8.00	324	0.20	3
A2	Gas transmission pipeline	API 5L X70	762	10.50	12.30	9.00	350	0.28	3
A3	Multiphase flowline	API 5L X60	406	7.00	8.40	6.50	290	0.35	2
A4	Pressure separator cylindrical shell	Carbon steel	1200	5.50	16.10	12.00	240	0.15	2
A5	Compressor discharge line	API 5L X65	323.9	11.00	7.40	5.50	324	0.32	1
A6	Offshore export pipeline	API 5L X65	914	9.50	13.10	9.50	324	0.25	4

Deterministic Wall-Loss and Hoop-Stress Screening Model

For each asset i, remaining wall thickness $t_i(\tau)$ after τ years ($\tau = 0$, 5 and 10) was calculated using a constant-rate uniform wall-loss model, with D and P held constant:

$$t_i(\tau) = t_{0,i} - \mathrm{CR}_i\,\tau \tag{1}$$

Before stress evaluation, initial geometry was checked against the thin-wall criterion $\frac{D_i}{t_{0,i}} \geq 20$. Nominal hoop stress $\sigma_{h,i}(\tau)$ was then calculated using the mean-diameter formulation $D_m = D_i - t_i(\tau)$:

$$\sigma_{h,i}(\tau) = \frac{P_i[D_i - t_i(\tau)]}{2\,t_i(\tau)} \tag{2}$$

Hoop-stress utilisation $U_{\sigma,i}(\tau; E_i)$ and the remaining thickness margin $M_{t,i}(\tau)$ were evaluated separately using Equations (3) and (4):

$$U_{\sigma,i}(\tau; E_i) = \frac{\sigma_{h,i}(\tau)}{E_i\,S_{\text{allow},i}} \tag{3}$$

$$M_{t,i}(\tau) = t_i(\tau) - t_{\min,i} \tag{4}$$

Here, E_i denotes the weld joint-efficiency factor. Baseline cases were evaluated at $E_i = 1.00$, while separator shell A4 was also assessed at $E = 0.90$ and $E = 0.85$ to examine sensitivity to design-code assumptions. Setting nominal stress utilisation to unity gives the stress-governed minimum-thickness threshold $t_{\sigma,i}$:

$$t_{\sigma,i} = \frac{P_i D_i}{2\,E_i S_{\text{allow},i} + P_i} \tag{5}$$

Deterministic compliance at horizon τ was defined using a binary indicator $H_i(\tau)$, assigned a value of one only when both minimum wall-thickness and hoop-stress limits were satisfied:

$$H_i(\tau) = \begin{cases} 1, & \text{if } t_i(\tau) > t_{\min,i} \text{ and } U_{\sigma,i}(\tau) < 1 \\ 0, & \text{if } t_i(\tau) \leq t_{\min,i} \text{ or } U_{\sigma,i}(\tau) \geq 1 \end{cases} \tag{6}$$

Probabilistic Reliability Formulation and Monte Carlo Simulation

To assess the uncertainty propagated over the selected horizons, four input parameters were modelled as statistically independent random variables in the vector $\mathrm{X} = [P, S^*, T_0, C]$: operating pressure, screening resistance, initial wall thickness and corrosion rate, respectively. Outside diameter (D), minimum screening thickness ($t_{\min}$) and weld joint-efficiency factor (E) were treated as deterministic parameters. Diameter was fixed as a modelling assumption to isolate the effects of the four stochastic

inputs. Their prescribed distributions, reference means and coefficients of variation (CoVs) are given in Table 2.

Table 2. Stochastic input distributions and deterministic parameters for Monte Carlo screening

Variable	Symbol	Unit	Distribution	Mean (μ)	CoV	Modelling rationale
Operating pressure	P	MPa	Normal	P_{ref}	0.04	Captures minor steady-state pressure fluctuations
Screening resistance	$S^{\star}$	MPa	Lognormal	S_{allow}	0.06	Non-negative; reflects screening-resistance variability
Initial wall thickness	T_0	mm	Normal	t_0	0.02	Accounts for fabrication and baseline ultrasonic thickness (UT) measurement uncertainty
Corrosion rate	C	mm/yr	Lognormal	CR	0.20	Enforces non-negative loss; moderate rate scatter
Outside diameter	D	mm	Deterministic	D_{ref}	—	Nominal geometry held constant
Minimum thickness	$t_{\min}$	mm	Deterministic	$t_{\min,\text{ref}}$	—	Prescribed code/screening limit
Weld joint factor	E	—	Deterministic	1.00; 0.90; 0.85	—	Fixed scenario parameter (sensitivity for A4 only)

For normally distributed variables (P and T_0), standard deviations were calculated as $\sigma = \mu\,\text{CoV}$. The normal distributions were not truncated because the small CoVs (0.04 and 0.02) make non-positive draws extremely unlikely ($\ll 10^{-100}$). For lognormal variables (S^* and C) with arithmetic mean m and coefficient of variation c, the underlying log-space parameters were calculated as $\mu_{\ln} = \ln(m) - \frac{1}{2}\ln(1+c^2)$ and $\sigma_{\ln} = \sqrt{\ln(1+c^2)}$.

At horizon τ, stochastic remaining thickness $T(\tau)$ and hoop stress $\sigma_h(\mathbf{X},\tau)$ are given by:

$$T(\tau) = T_0 - C\,\tau, \qquad \sigma_h(\mathbf{X},\tau) = \frac{P[D - T(\tau)]}{2\,T(\tau)} \tag{7}$$

The thickness and hoop-stress limit-state functions are defined as:

$$g_1(\mathbf{X},\tau) = T(\tau) - t_{\min} \tag{8}$$

$$g_2(\mathbf{X},\tau;E) = E\,S^{\star} - \sigma_h(\mathbf{X},\tau) \tag{9}$$

Any realisation producing $T(\tau) \le 0$, $g_1 \le 0$ or $g_2 \le 0$ was classified as a threshold exceedance. Joint screening reliability $R(\tau;E)$ represents the probability that both limit states are satisfied:

$$R(\tau;E) = \Pr[g_1(\mathbf{X},\tau) > 0 \ \wedge\ g_2(\mathbf{X},\tau;E) > 0] \tag{10}$$

For each asset, $N = 1{,}000{,}000$ Monte Carlo realisations were generated with NumPy's default_rng(seed=42), initialised once and applied sequentially from A1 to A6. For each asset, 10^6 independent samples were drawn in the specified order P (normal), S^* (lognormal), T_0 (normal) and C (lognormal), then evaluated at all three horizons ($\tau = 0$, 5 and 10 years). For separator shell A4, the same sample set was evaluated at $E = 1.00$, 0.90 and 0.85. Monte Carlo reliability was estimated from the indicator mean:

$$\hat{R}(\tau;E) = \frac{1}{N}\sum_{k=1}^{N} \mathbb{I}\left[g_{1,k}(\tau) > 0 \ \wedge\ g_{2,k}(\tau;E) > 0\right] \tag{11}$$

Here, $\mathbb{I}[\cdot]$ equals one when both conditions are satisfied and zero otherwise. The Monte Carlo standard error was calculated as $\mathrm{SE} = \sqrt{\frac{\hat{R}(1-\hat{R})}{N}}$, yielding a maximum standard error of 0.0005 and a 95% sampling half-width not exceeding 0.001 at $N = 10^6$.

Inter-Horizon Reliability Decay Metrics

To quantify the change in reliability between five and ten years, four measures were calculated from the unrounded Monte Carlo estimates: absolute reliability decline (ΔR), five-to-ten-year retention percentage, annual absolute decline (d) and logarithmic interval decay coefficient (k):

$$\Delta R = R_5 - R_{10}, \qquad \text{Retention (\%)} = 100\left(\frac{R_{10}}{R_5}\right) \tag{12}$$

$$d = \frac{\Delta R}{5}, \qquad k = \frac{1}{5}\ln\left(\frac{R_5}{R_{10}}\right) \tag{13}$$

For $R_5 > 0$ and $R_{10} > 0$, the exponential relation $R(\tau) = R_5 \exp[-k(\tau - 5)]$ describes inter-horizon reliability decay over $\tau \in [5,10]$ years. Assets were ranked independently at $\tau = 5$ and $\tau = 10$ years in descending order of joint screening reliability.

RESULTS

Deterministic Wall-Thickness and Stress Screening

All six benchmark assets satisfied the thin-wall criterion ($\frac{D}{t_0} \geq 20$) at the reference condition, with initial ratios ranging from 43.8 (A5) to 74.5 (A4) (Table 3). Under deterministic constant-rate wall loss, threshold exceedances occurred at different horizons across the portfolio. At baseline ($\tau = 0$ years), A6 exceeded the nominal hoop-stress limit ($U_\sigma = 1.008$), whereas all other assets remained within both limits ($U_\sigma \leq 0.914$). At five years ($\tau = 5$), A2 crossed the stress threshold ($U_\sigma = 1.034$), alongside A6 ($U_\sigma = 1.116$). All assets are positive thickness margins above $t_{\min}$, although the margins narrowed to 0.15 mm for A3 and 0.30 mm for A5. At ten years ($\tau = 10$), only A1 and A4 remained free of deterministic threshold exceedances (flag N). A3 breached its minimum-thickness limit ($t = 4.90$ mm < 6.50 mm; flag T), A5 exceeded both thickness and stress limits ($t = 4.20$ mm, $U_\sigma = 1.292$; flag ST), and A2 and A6 remained stress-governed (S).

Table 3. Deterministic wall thickness and mean-diameter hoop-stress utilisation (E = 1.00)

Asset	$\frac{D}{t_0}$	0 yr: t (mm); U_σ	5 yr: t (mm); U_σ	10 yr: t (mm); U_σ	Active flags (0 / 5 / 10 yr)
A1	56.5	10.80; 0.685	9.80; 0.756	8.80; 0.843	N / N / N
A2	62.0	12.30; 0.914	10.90; 1.034	9.50; 1.188	N / S / S
A3	48.3	8.40; 0.571	6.65; 0.725	4.90; 0.988	N / N / T
A4	74.5	16.10; 0.843	15.35; 0.884	14.60; 0.930	N / N / N
A5	43.8	7.40; 0.726	5.80; 0.931	4.20; 1.292	N / N / ST
A6	69.8	13.10; 1.008	11.85; 1.116	10.60; 1.249	S / S / S

Note. N = no threshold exceeded; S = hoop-stress limit exceeded; T = minimum-thickness limit exceeded; ST = both thresholds exceeded.

Multi-Horizon Probabilistic Reliability and Rank Dynamics

Joint screening reliability (R_τ) decreased monotonically across all six assets between $\tau = 0$ and $\tau = 10$ years, with Monte Carlo standard errors below 0.0005 for $N = 1{,}000{,}000$ trials (Table 4). At baseline ($\tau = 0$), A1, A3 and A5 recorded reliabilities that round to 1.0000. For A5, eight exceedances occurred in 10^6 trials ($R_0 = 0.999992$ before rounding), whereas A6 began below 0.5 ($R_0 = 0.4488$).

Table 4. Monte Carlo joint screening reliability estimates (N = 1,000,000 per asset)

Asset	R_0	R_5	R_{10}	SE(R_5)	SE(R_{10})	Nominal 10-yr flag
A1	1.0000	0.9998	0.9328	0.00001	0.00025	N
A2	0.8808	0.3331	0.0308	0.00047	0.00017	S
A3	1.0000	0.6753	0.0029	0.00047	0.00005	T
A4	0.9887	0.9460	0.8165	0.00023	0.00039	N
A5	1.0000	0.7005	0.0061	0.00046	0.00008	ST
A6	0.4488	0.0776	0.0049	0.00027	0.00007	S

As illustrated in Figure 1, the reliability estimates diverged markedly between five and ten years: A1 ($R_{10} = 0.9328$) and A4 ($R_{10} = 0.8165$) retained over 86% of their five-year compliance probabilities, whereas A2, A3, A5 and A6 fell below 0.031 by year ten (Table 5). These differences were accompanied by changes in relative rank. A3 and A5 showed the largest absolute reliability declines ($\Delta R = 0.6725$ and 0.6944) and the highest logarithmic decay coefficients ($k = 1.0936\ \mathrm{yr}^{-1}$ and $0.9486\ \mathrm{yr}^{-1}$), falling from fourth and third at year five to sixth and fourth at year ten, respectively. A2 rose from fifth to third at year ten despite retaining only 9.3% of its five-year reliability.

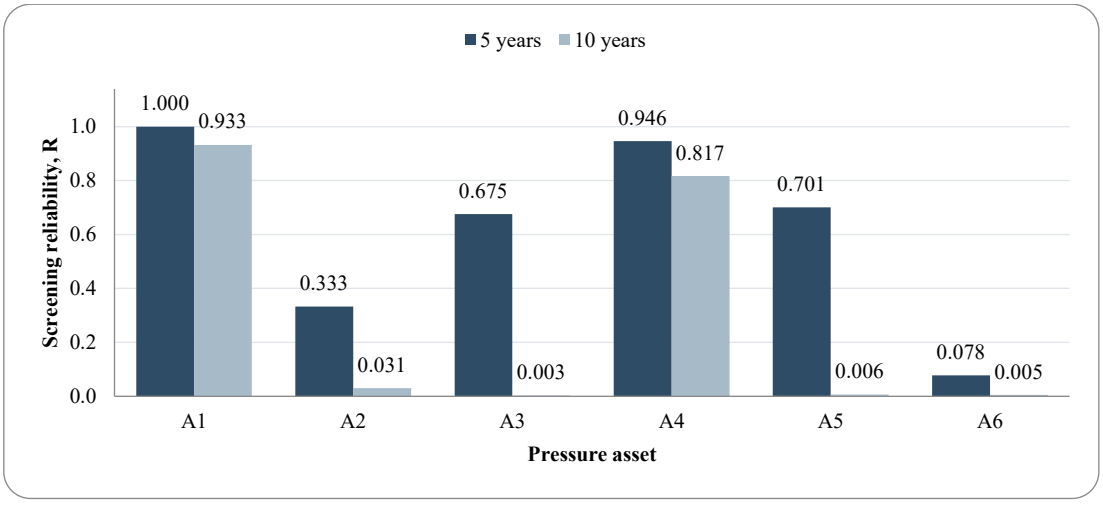


Figure 1. Five- and ten-year joint screening-reliability estimates (R_5 and R_{10}) across assets A1–A6 ($N = 1{,}000{,}000$ realisations per asset).

Table 5. Paired-horizon reliability decay metrics and ordinal portfolio rankings

Asset	R_5	R_{10}	ΔR	Retention (%)	d (yr^{-1})	k (yr^{-1})	Rank (5 yr)	Rank (10 yr)
A1	0.9998	0.9328	0.0670	93.3	0.0134	0.0139	1	1
A2	0.3331	0.0308	0.3022	9.3	0.0604	0.4760	5	3
A3	0.6753	0.0029	0.6725	0.4	0.1345	1.0936	4	6

Asset	R_5	R_{10}	ΔR	Retention (%)	d (yr^{-1})	k (yr^{-1})	Rank (5 yr)	Rank (10 yr)
A4	0.9460	0.8165	0.1295	86.3	0.0259	0.0294	2	2
A5	0.7005	0.0061	0.6944	0.9	0.1389	0.9486	3	4
A6	0.0776	0.0049	0.0727	6.3	0.0145	0.5515	6	5

Note. Absolute decline (ΔR), retention percentage, annual absolute decline (d) and logarithmic interval decay coefficient (k) were calculated from unrounded Monte Carlo estimates before table rounding.

Sensitivity of Separator Shell Compliance to Joint Efficiency

Reducing the weld joint-efficiency factor (E) for the pressure-separator shell (A4) substantially increased nominal hoop-stress utilisation and reduced joint compliance across the assessed horizons (Table 6). At $E = 0.90$, nominal stress utilisation remained below unity at baseline (0.936) and year five (0.983), but exceeded unity at year ten (1.034); R_{10} decreased from 0.8165 to 0.3290. At $E = 0.85$, nominal stress utilisation exceeded unity by year five (1.040) and reached 1.094 at year ten, reducing R_{10} further to 0.1205.

Table 6. Screening sensitivity of pressure-separator shell (Asset A4) to weld joint-efficiency factor (E)

E	Nominal $U_{\sigma,0}$	Nominal $U_{\sigma,5}$	Nominal $U_{\sigma,10}$	R_5	R_{10}
1.00	0.843	0.884	0.930	0.9460	0.8165
0.90	0.936	0.983	1.034	0.5831	0.3290
0.85	0.991	1.040	1.094	0.2943	0.1205

DISCUSSION

Divergence of Governing Limit States Across Horizons

Threshold exceedances occurred in different ways across the six pressure-asset benchmarks: stress- and thickness-governed exceedances occurred at different stages of service life (Tables 3 and 4; Figure 1). A6 exceeded its nominal hoop-stress threshold at the reference condition ($U_\sigma = 1.008$ at $\tau = 0$), with a low five-year joint-compliance probability ($R_5 = 0.0776$). Meanwhile, A3 satisfied both checks through year five, but had fallen below its minimum wall thickness requirement by year ten ($t = 4.90$ mm < 6.50 mm), which produced the lowest ten-year portfolio reliability ($R_{10} = 0.0029$). These differences relate to differences in geometry, operating pressure and available wall-thickness margin (Table 1): the larger diameter-to-thickness ratio ($D/t_0 = 69.8$ vs. 48.3) and higher operating pressure (9.50 vs. 7.00 MPa) pushed A6 above its nominal stress threshold at baseline, whereas the lower operating pressure and increased corrosion rate (0.35 mm/yr vs. 0.25 mm/yr) drained away the 1.90 mm initial wall-thickness margin of A3 by year ten.

Inter-Horizon Decay Kinetics and Portfolio Rank Reversals

Joint screening reliability for each asset decreased between years five and ten, but the assets' relative ranks shifted at this interval (Table 5; Figure 1). Most notably, A2, which was ranked fifth at year five, rose to third place at year ten, even though this asset lost over 90% of its five-year reliability ($R_5 = 0.3331$ versus $R_{10} = 0.0308$; $\Delta R = 0.3022$). This upward trend does not indicate that A2 had stabilised; rather, A3 and A5 degraded faster than A2 during the second five-year period, with their logarithmic decay rate coefficients $k_{A3} = 1.0936\ yr^{-1}$ and

k_{A5} = 0.9486 yr^{-1} being greater than that of A2 (k_{A2} = 0.4760 yr^{-1}). The joint reliability of A3 and A5 dropped below that of A2 as the screening margins narrowed (Tables 3 and 5). This concurs with results from corrosion-maintenance research showing that assessment windows and limit-state definitions can influence asset rankings based on relative rankings (De-León-Escobedo, 2023; A. Li et al., 2024). Relative ranks alone can mask large absolute reliability declines (ΔR) and the proportional change represented by the interval coefficient (k), which should be taken into account in maintenance planning to set follow-up priorities for assets such as A3 and A5.

Sensitivity to Prescriptive Design Assumptions

Considering the cylindrical separator shell (A4) at lower weld joint-efficiency factors shows the effect of the design-code assumptions for long-term screening (Table 6). The ten-year screening reliability (R 10) at E = 1.00 was 0.8165; at E = 0.90 and 0.85 R 10 was reduced to 0.3290 and 0.1205, respectively, while the nominal ten-year stress utilization increased from 0.930 to 1.034 and 1.094. Because joint efficiency determines the maximum screening resistance, the reduced E lowers the difference between the operating hoop stress and material resistance, with no alteration in physical wall loss. At the defined pressure and resistance uncertainty, the 15% decrease in E decreased the simulated 10-year passing probability to 0.1205. These results are consistent with related pressure-vessel investigations that demonstrated the effect of resistance formulations and shell geometry on integrity assessment (Pascal, 2026b; Zhu et al., 2023). This shows how a presumed joint-efficiency factor can impact the screening process of an ageing vessel when fabrication records are incomplete. The two-horizon process facilitates preliminary asset triage prior to detailed engineering evaluation. By isolating A6's baseline stress exceedance, tightening of the thickness margins for A3 and A5, and the sensitivity of A4 to weld joint efficiency, operators can identify those assets requiring ILI, ultrasonic thickness mapping or equipment-specific FFS assessment.

CONCLUSION

This paper introduced a preliminary, two-horizon (deterministic and probabilistic) screening methodology for corrosion-induced wall loss in six upstream hydrocarbon pressure assets. The use of two different severity measures (minimum wall-thickness and mean-diameter hoop-stress limits) distinguished baseline stress-limit exceedances (U_σ = 1.008 at τ = 0) from longer-term wall-thickness violations (A3: 4.90 mm versus a 6.50 mm minimum at ten years), while the probabilistic analysis distinguished short-term screening reliability from longer-term reliability decline under statistically independent, asset-specific input uncertainties. Sensitivity testing of the cylindrical pressure-separator shell (A4) revealed that long-term reliability is sensitive to the assumed weld-joint efficiency. The use of relative change in screening reliability between five and ten years tracked changes in portfolio ranking as the reliability of individual assets declined, using the logarithmic interval decay coefficient (k). Absolute change in screening reliability (ΔR) can further distinguish the magnitude of reliability loss between assets when considered alongside their estimated reliability at the assessed horizons. Future studies can be extended to track deterministic and probabilistic component reliability of corroded assets over multiple inspection intervals, to examine dependencies between input parameters, and to assess how screening probabilities could support fitness-for-service (FFS)-based risk-based inspection (RBI) planning.

REFERENCES

Amaya-Gómez, R., Sánchez-Silva, M., Muñoz, F., Schoefs, F., & Bastidas-Arteaga, E. (2024). Spatial characterization and simulation of new defects in corroded pipeline based on in-line inspections. *Reliability Engineering & System Safety, 241*, Article 109697. https://doi.org/10.1016/j.ress.2023.109697

Amaya-Gómez, R., Schoefs, F., Sánchez-Silva, M., Muñoz, F., & Bastidas-Arteaga, E. (2022). Matching of corroded defects in onshore pipelines based on in-line inspections and Voronoi partitions. *Reliability Engineering & System Safety, 223*, Article 108520. https://doi.org/10.1016/j.ress.2022.108520

American Petroleum Institute. (2022). *Pressure vessel inspection code: In-service inspection, rating, repair, and alteration* (API Standard 510, 11th ed.). https://www.api.org/products-and-services/standards/important-standards-announcements/standard510

American Petroleum Institute. (2024). *Piping inspection code: In-service inspection, rating, repair, and alteration of piping systems* (API Standard 570, 5th ed.). https://www.api.org/products-and-services/standards/important-standards-announcements/std570

American Society of Mechanical Engineers. (2023). ASME B31G-2023: Manual for determining the remaining strength of corroded pipelines. https://www.asme.org/codes-standards/find-codes-standards/b31g-manual-determining-remaining-strength-corroded-pipelines/2023

American Society of Mechanical Engineers. (2025). *Boiler and pressure vessel code, Section VIII, Division 1: Rules for construction of pressure vessels* (BPVC.VIII.1–2025). https://www.asme.org/codes-standards/find-codes-standards/bpvc-viii-1-bpvc-section-viii-rules-construction-pressure-vessels-division-1

Boufkhed, H., Laggoune, R., Amaya-Gómez, R., & Bastidas-Arteaga, E. (2026). Spatio-temporal assessment of the reliability of corroded pipeline considering time-dependent failure modes. *Corrosion and Materials Degradation, 7*(4), Article 59. https://doi.org/10.3390/cmd7040059

Cui, B., & Wang, H. (2024). Pipeline corrosion prediction and uncertainty analysis with an ensemble Bayesian neural network approach. *Process Safety and Environmental Protection, 187*, 483–494. https://doi.org/10.1016/j.psep.2024.05.011

Dao, U., Sajid, Z., Khan, F., Zhang, Y., & Tran, T. (2023). Modeling and analysis of internal corrosion induced failure of oil and gas pipelines. *Reliability Engineering & System Safety, 234*, Article 109170. https://doi.org/10.1016/j.ress.2023.109170

De-León-Escobedo, D. (2023). Risk-based maintenance time for oil and gas steel pipelines under corrosion including uncertainty on the corrosion rate and consequence-based target reliability. *International Journal of Pressure Vessels and Piping, 203*, Article 104927. https://doi.org/10.1016/j.ijpvp.2023.104927

DNV. (2025). *DNV-RP-F101: Corroded pipelines* (September 2019 edition, amended September 2025). https://www.dnv.com/energy/standards-guidelines/dnv-rp-f101-corroded-pipelines/

Hsu, Y. S. (2024). Subset simulation based simplified approach for pipeline with multiple irregular corrosion defects in time-dependent reliability analysis. *International Journal of Pressure Vessels and Piping, 211*, Article 105295. https://doi.org/10.1016/j.ijpvp.2024.105295

Huang, Y., Qin, G., & Yang, M. (2023). A risk-based approach to inspection planning for pipelines considering the coupling effect of corrosion and dents. *Process Safety and Environmental Protection, 180*, 588–600. https://doi.org/10.1016/j.psep.2023.10.025

Hussain, M., & Zhang, T. (2025). Machine learning-based outlier detection for pipeline in-line inspection data. *Reliability Engineering & System Safety, 254*, Article 110553. https://doi.org/10.1016/j.ress.2024.110553

Hussain, M., Zhang, T., Dwight, R., & Jamil, I. (2024). Energy pipeline degradation condition assessment using predictive analytics challenges, issues, and future directions. *Journal of Pipeline Science and Engineering, 4*(3), Article 100178. https://doi.org/10.1016/j.jpse.2024.100178

Li, A., Jin, F., Li, Y., Lan, W., Liu, P., Yu, Z., & Wen, K. (2024). A reliability assessment method for natural gas pipelines with corroded defects that considers detection cycles. *Energies, 17*(14), Article 3366.

Li, C., Yang, F., Jia, W., Liu, C., Zeng, J., Song, S., & Zhang, Y. (2023). Pipelines reliability assessment considering corrosion-related failure modes and probability distributions characteristic using subset simulation. *Process Safety and Environmental Protection, 178*, 226–239. https://doi.org/10.1016/j.psep.2023.08.013

Li, H., Huang, K., Zeng, Q., & Sun, C. (2022). Residual strength assessment and residual life prediction of corroded pipelines: A decade review. *Energies, 15*(3), Article 726. https://doi.org/10.3390/en15030726

Ma, H., Zhang, W., Wang, Y., Ai, Y., & Zheng, W. (2023). Advances in corrosion growth modeling for oil and gas pipelines: A review. *Process Safety and Environmental Protection, 171*, 71–86. https://doi.org/10.1016/j.psep.2022.12.054

Mensah, A., & Sriramula, S. (2024). Probabilistic finite element-based reliability of corroded pipelines with interacting corrosion cluster defects. *International Journal of Pressure Vessels and Piping, 207*, Article 105086. https://doi.org/10.1016/j.ijpvp.2023.105086

NACE International. (2016). *International measures of prevention, application, and economics of corrosion technologies study*. https://www.teke.fi/nace/Nace-International-Report.pdf

Nahal, M., Sahraoui, Y., Khelif, R., & Chateauneuf, A. (2023). System reliability of corroded pipelines considering spatial and stochastic dependency in irregular zones. *Gas Science and Engineering, 117*, Article 205083. https://doi.org/10.1016/j.jgsce.2023.205083

Pascal, M. A. (2026a). Machine learning approach for remaining useful life prediction for oil pipelines under data scarcity: A risk-based inspection framework. *Proceedings of the Institution of Mechanical Engineers, Part E: Journal of Process Mechanical Engineering*. Advance online publication. https://doi.org/10.1177/09544089261484737

Pascal, M. A. (2026b). Thickness probabilistic and deterministic prediction models for enhancing risk-based inspection for structure integrity and failure prevention. *ASCE-ASME Journal of Risk and Uncertainty in Engineering Systems, Part B: Mechanical Engineering, 12*(2), Article 021103. https://doi.org/10.1115/1.4070309

Pipeline and Hazardous Materials Safety Administration. (2018a). *Fact sheet: Corrosion*. https://primis.phmsa.dot.gov/stakeholder-comms/factsheets/fscorrosion/

Pipeline and Hazardous Materials Safety Administration. (2018b). *Fact sheet: Internal corrosion*.https://primis.phmsa.dot.gov/stakeholder-comms/factsheets/fsinternalcorrosion/

Velázquez, J. C., Hernández-Sánchez, E., Terán, G., Capula-Colindres, S., Diaz-Cruz, M., & Cervantes-Tobón, A. (2022). Probabilistic and statistical techniques to study the impact of localized corrosion defects in oil and gas pipelines: A review. *Metals, 12*(4), Article 576. https://doi.org/10.3390/met12040576

Velázquez, J. C., Valor, A., & Caleyo, F. (2024). Statistical study of localized internal corrosion defects in oil and gas pipelines through sampling inspection. *Process Safety and Environmental Protection, 186*, 566–576. https://doi.org/10.1016/j.psep.2024.04.020

Zerouali, B., Sahraoui, Y., Nahal, M., & Chateauneuf, A. (2024). Reliability-based maintenance optimization of long-distance oil and gas transmission pipeline networks. *Reliability Engineering & System Safety, 249*, Article 110236. https://doi.org/10.1016/j.ress.2024.110236

Zhu, X.-K., Wiersma, B. J., Johnson, W. R., & Sindelar, R. (2023). Burst pressure solutions of thin and thick-walled cylindrical vessels. *Journal of Pressure Vessel Technology, 145*(4), Article 041303. https://doi.org/10.1115/1.4062334